Available online at www.sciencedirect.com

ScienceDirect

journal homepage: www.elsevier.com/locate/he

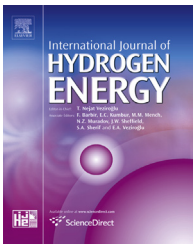

Evaluation and optimization of the alkaline water electrolysis ohmic polarization: Exergy study

Khalid Zouhri [a,b,*], *Seong-young Lee* [a]

[a] *Department of Mechanical Engineering-Engineering Mechanics, Michigan Technological University, 1400 Townsend Dr., Houghton, MI 49931, USA*

[b] *Department of Mechanical Engineering, University of New Haven, 300 Boston Post Road, West Haven, CT 06516, USA*

ARTICLE INFO

Article history:
Received 11 February 2016
Received in revised form
21 March 2016
Accepted 21 March 2016
Available online 13 April 2016

Keywords:
Water electrolysis
Exergy
Energy
Ohmic overpotential
Ionic conductivity
Hydrogen bubbles

ABSTRACT

A model is created in order to investigate the effect of different material parameters on the ohmic overpotential of the alkaline water electrolysis for hydrogen production, which influences the exergy efficiency of the water electrolysis. In this research, it was demonstrated that the electrode material parameters and electrolyte conditions of the water electrolysis components such as electrode and membrane resistivity, distance between the electrodes, oxygen and hydrogen bubbles that covers the electrode surface, electrolyte concentration, electrolyte ionic conductivity, and temperature have various effects on the ohmic overpotential, which consequently affect the exergy efficiency of the alkaline water electrolysis. The results of our model has illustrated that the highest exergy loss is due to hydrogen bubbles followed by the electrolyte ionic resistance and oxygen bubbles resistance, respectively. The model has also provided a strong direction for how to optimize the exergy efficiency by reducing the ohmic overpotential, which is affected by various material parameters and operating conditions.

Introduction

The environmental pollution and the diminution of fossil fuel have increased the interest of the research and development of renewable energy technologies. Hydrogen is the most abundant element in the universe, is considered to be environmentally friendly and to have high energy density. On planets such as Earth, hydrogen is found as part of the molecules of water, organic material, and natural gas. Hydrogen is expected to play an important role in the near future especially as an energy carrier for sustainable research and development. Water electrolysis is a well-known process and is currently adopted in many applications in order to produce hydrogen with high purity [1,2]. Water electrolysis is particularly suitable for use in combination with photovoltaics (PVs) because hydrogen production by electrolysis of water is a mature and efficient technology. Various technologies are available to produce hydrogen via water electrolysis.

The most common water electrolysis is alkaline water electrolysis, polymer exchange membranes (PEM), and solid oxides. The concept is the same for most technologies, which

* *Corresponding author*. Department of Mechanical Engineering-Engineering Mechanics, Michigan Technological University, 1400 Townsend Dr., Houghton, MI 49931, USA. Tel.: +1 203 931 5715; fax: +1 203 306 3055.
E-mail address: kzouhri@mtu.edu (K. Zouhri).

http://dx.doi.org/10.1016/j.ijhydene.2016.03.119

Nomenclature

A	Area, cm^2
C	Coulomb, C
c	The Concentration of dissolved gas, mol m^{-3}
D_v	diffusion coefficient, $cm^2\ s^{-1}$
d	Bubble diameter, cm
E	electrode potential, V
E_{act}	activation overpotential, V
E_{rev}	ohmic overpotential, V
F_o	Fourier number
F	Faraday's constant, C mol^{-1}
f	volume fraction
f_G	gas evolution efficiency
G	Gibbs free energy, kJ
i	current density, mA cm^{-2}
i_o	exchange current density, mA cm^{-2}
H	enthalpy, kJ
K_d	the apparent conductivity, S cm^{-1}
k_{water}	the specific conductivity, S cm^{-1}
L	length, cm
m	the hydraulic radius, cm
M	molecular weight, g mol^{-1}
n	number of moles of electrons

Greek symbol

α	transfer coefficient
α_{act}	the activation transfer coefficient
θ	gas bubble surface coverage percentage, %
ε_b	efficiency
η	overpotential, V
η_{ohm}	ohmic polarization, V

Subscript

ele	electrolyte
m	membrane
Ohm	ohmic
w	water
p	partial pressure, kPa
P	pressure, kPa
Q	electrical charge, C
Q_j	the heat loss, kJ
R_g	universal gas constant 8.314 J $mol^{-1}\ K^{-1}$
R_e	Reynolds number
R	electrical resistance, Ω
R_{ions}	ionic resistances, Ω
R_1	the electrical circuit resistance (External), Ω
R'_1	wiring and connections electrical resistance, Ω
$R_{bubble;O2}$	oxygen bubbles resistance, Ω
$R_{membrane}$	membrane resistance, Ω
R_{anode}	anode resistance, Ω
R_b	Bubble radius, cm
S_{gen}	the entropy generation, kJ
r	production rate, $m^3\ h^{-1}$
T_{amb}	the ambient temperature, K
t	time, s
U	electrical voltage, V
V_r	bubble volume, cm^3
V_G	volume rate of evolved gas, $cm^3\ s^{-1}$
η_{act}	activation polarization, V
ρ_j	the resistivity of component j, Ω cm
σ_o	the interface conductivity, S cm^{-1}
σ_{el}	electronic conductivity, S cm^{-1}
σ_{io}	ionic conductivity, S cm^{-1}

Superscript

rev	reversible
t,n	thermoneutral
act	activation

is two electrodes and an electrolyte that allows the transport of ions. The alkaline water electrolysis usually operates with electrolyte concentrated with NaOH or KOH. The operating temperature for alkaline water electrolysis and PEM water electrolysis is between 60 and 90 °C, while the solid oxide is between 600 and 900 °C. The alkaline water electrolysis has been widely used in industrial application and for a large number of built units already in operation, while the PEMs water electrolysis still have limited application in terms of production capacity because of the limited lifetime and corrosion of the cells [3,4]. Hydrogen can be produced using a number of different processes such as water electrolysis, thermochemical process, and direct solar water splitting process [5]. Currently, hydrogen is mostly being produced from fossil fuels such as natural gas, coal and oil, using the following thermochemical process: steam reforming, gasification, and partial oxidation. The most frequently used process is the catalytic steam reforming of natural gas and coal gasification.

The water electrolysis process carries significantly higher costs than hydrogen production from fossil fuels [6]. Hydrogen production via water electrolysis process represents less than 5% of world hydrogen production [7], which is used for small scale hydrogen production whereas large-scale hydrogen production is prohibitively expensive or impossible to implement with usages such as spacecraft. The alkaline water electrolysis has many generous advantages such as flexibility, availability, and high purity compared to the thermochemical processes (steam reforming or coal gasification) [8]. While possessing these advantages, hydrogen production via water electrolysis still required improvement in the efficiency and cost of the material and installations, and for this reason we are performing our study on the effect of the materials' parameters and water electrolysis geometry and conditions on the alkaline water electrolysis exergy efficiency.

The alkaline water electrolysis has two types of losses [9]: ohmic overpotential and activation overpotential. The ohmic polarization is caused by the electrodes' resistance, electrolyte resistance, membrane resistance, internal connection wire resistance, and hydrogen and oxygen bubbles resistance. The most critical factors governing the ohmic losses in alkaline water electrolysis are the electrode and membrane material resistivity, electrolyte conductivity and concentration, and electrode and electrolyte geometry. Activation polarization is the voltage overpotential required to overcome the activation energies of the electrochemical reactions on

the anode and cathode surfaces. In this work, the analysis of the effect of material properties and operating condition variations is performed only on the ohmic overpotential. The water electrolysis exergy efficiency is affected by many factors—such as temperature, pressure, electrodes resistivity, distance between the electrodes, membrane permeability, membrane resistivity, electrolyte ionic conductivity, electrolyte concentration, etc. Fewer results [10,11] were reported on the activation polarization of the alkaline water electrolysis. Jaroslaw el al. has investigated the Influence of pressure and temperature on the value of reversible electrolysis voltage and activation polarization, also Kai el al. has investigated the effect temperature on the activation polarization and ionic conductivity of the electrolyte. Both models have investigated the effect of operating conditions on the activation polarization of the alkaline water electrolysis; Also, Marini el al. [12] has demonstrated that the effect of pressure differentials in a recirculating electrolyte scheme helps reduce mass transport limitations (activation polarization), increasing efficiency and power density. Moreover, other studies [13–18] on the operating condition effect on the activation polarization of the alkaline water electrolysis were reported; however, they did not discussed the effect of material parameters on the ohmic polarization as well its effect on the exergy efficiency of the alkaline water electrolysis. Therefore, to the best of our knowledge, the effect of materials properties on the ohmic polarization and its effect on the exergy efficiency have not been presented in the open literature. This is important because the effect of the electrodes and membrane materials' parameters and water electrolysis geometry has not previously been understood to consider the effect of those factors on ohmic polarization and its effect on the exergy efficiency. To this end, this work presents a comprehensive analysis to understand the impact of each factor on the exergy efficiency of the water electrolysis. The aim of this paper is to understand the parameters that influence the ohmic polarization and how it can be optimized to reduce the water electrolysis losses and enhance the exergy efficiency.

Electrochemical model

The water electrolysis process consists of cathode, anode, and ion-conducting electrolyte [4] as described in Fig. 1 below. Hydrogen and oxygen are produced at the cathode and the anode, respectively.

The chemical reaction for the alkaline water electrolysis is described by the following equation:

$$2H_2O + \text{Electricity} \rightarrow 2H_2 + O_2 \quad (1)$$

The reaction that occurs at the anode side can be described by the following:

$$2OH^- \rightarrow H_2O + 0.5O_2 + 2e^- \quad (2)$$

The reaction occurs at the cathode side can be described as follows:

$$2H_2O + 2e^- \rightarrow 2OH^- + H_2 \quad (3)$$

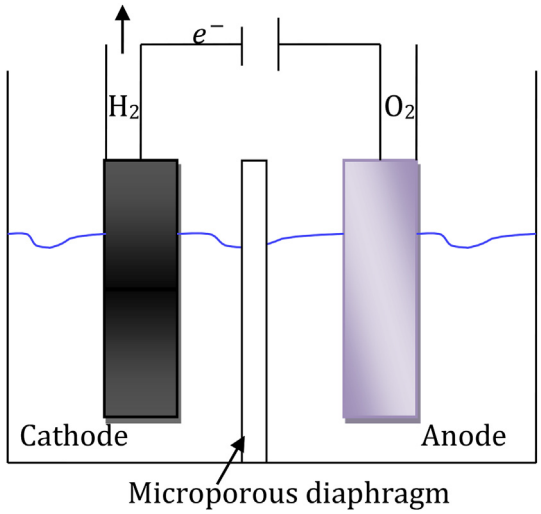

Fig. 1 – Schematic diagram of water electrolysis.

The typical materials used for the cathode are Ni–Mo, Pt–Ce, or Pt–Sm and for the anode is Ni or Fe. Due to the poor ion conductivity of water, the electrolysis uses an aqueous alkaline electrolyte, such as NaOH or KOH at a weight percentage of 30%.

The alkaline water electrolysis consists in the molecular decomposition using direct electric current. For the water electrolysis reaction to progress, a number of barriers have to be overcome such as the activation energies, electrical resistance of the circuit, and bubble resistance. These barriers requiring a necessary electrical energy supply. The following equation is the polarization curve which is calculated as follows:

$$E = E_{rev} + E_{act}(i) + E_{ohm}(i) \quad (4)$$

The reversible voltage at standard pressure and given temperature can be calculated as follow according to [19]:

$$E_{t,po}^{rev} = 1.50342 - 9.956 \cdot 10^{-4} T + 2.5 \cdot 10^{-7} T^2 \quad (5)$$

The activation overpotential equations are listed in detail in Appendix 1. In this analysis we will only focus on the ohmic overpotential and its effect on the exergy efficiency.

The ohmic overpotential

The ohmic overpotential of the water electrolysis is caused by the resistance of the electrodes, electrolyte solution, membrane resistance, hydrogen and oxygen bubble resistance, and the resistance from the connection wires.

The ohmic overpotential can be calculated as follows:

$$E_{ohm} = R_{total} \cdot I \quad (6)$$

where R_{total} is the total resistance and it can be calculated as follows:

$$R_{total} = R_{bubble,O_2} + R_1 + R_{anode} + R_{ions} + R_{membrane} + R_{bubble,H_2} + R_1' + R_{cathode} \quad (7)$$

where R_{ions}, R_1, R_1', R_{bubble,H_2}, R_{bubble,O_2}, $R_{membrane}$, R_{anode}, $R_{cathode}$, are the following respectively: 1) Ionic resistances, 2) The electrical circuit resistance (External), 3) Wiring and connections electrical resistance, 4) Oxygen bubbles resistance, 5) Hydrogen bubble resistance 6) Membrane resistance, 7) Anode resistance, 8) Cathode resistance.

The anode and cathode resistance

The anode and cathode resistance is the resistance that is caused by the electrodes' materials, and it can be calculated using the physics equation as follows:

$$R = \frac{L\rho_i}{A} \tag{8}$$

where ρ is the resistivity of the material of the component i; A is the area, and L is the length.

The resistance Equation (8) is applied to calculate the resistance of the electrical circuit resistance (External and internal) including wiring and connections electrical resistance.

The ionic resistance

The ionic resistance is caused by the electrolyte solution, which is affected by the concentration of the KOH in the water, and it can be described by the following equation:

$$R_{ions} = \frac{L}{A_{tank}\sigma_{ele}/C} \tag{9}$$

where L is the length between anode and cathode, A_{tank} is the area of the tank, σ_{ele} is the electrical conductivity of the electrolyte, and C is the electrolyte concentration.

The ionic conductivity of the alkaline solution as a function of the electrolyte composition and temperature is calculated based on the following equation [20]:

$$\sigma = -2.041\cdot M - 0.0028\cdot M^2 + 0.001043\cdot M^3 + 0.005332\cdot M\cdot T + 207.2\cdot\frac{M}{T} - 0.0000003\cdot M^2\cdot T^2 \tag{10}$$

At lower molarity this equation is not valid for molarity above 8. The following correlation can express the ionic conductivity for molarity greater than 8:

$$\sigma = \frac{132.1}{\exp\left(0.01592\cdot(M-12.27)^2 + \frac{0.3819\cdot M+9.406}{RT}\right)} \tag{11}$$

The membrane resistance

The membrane resistance is caused by the membrane material resistivity and its permeability; it can be described by the following equation:

$$R_{membrane} = \frac{L_m}{A_m K_d} \tag{12}$$

where K_d, L_m, and A_m are the apparent conductivity, length, and area of the membrane respectively. The resistivity of the membrane can be calculated by the following equation [21]:

$$K_d = 0.272\cdot\frac{km^2}{p} \tag{13}$$

where m is the hydraulic radius and p is the permeability.

The hydrogen and oxygen bubble resistance

The hydrogen and oxygen bubble resistance is caused by the bubble that covers the electrodes' surface which creates a resistance, and this resistance can be estimated by the following equations:

$$R_{bubble,H_2} = \frac{L_{anode,cathode}}{A_{tank}\cdot k_{water}\cdot\left(1-1.5\cdot f_{g-w,H_2}\right)} \tag{14}$$

where f_{g-w,H_2} is the volume fraction of gas in the solution

$$R_{bubble,O_2} = \frac{L_{a-c}\cdot\rho_{resistivity}}{A_{tank}} \tag{15}$$

where $\rho_{resistivity}$ can be calculated by the following equation:

$$\rho_{resistivity} = \rho_o(1-\varnothing)^{-3/2} \tag{16}$$

where ∅ is the percentage of the bubble coverage the electrodes surfaces and ρ_o is the specific resistivity of the water electrolysis solution.

The bubble coverage has substantial effect on the performance of the electrodes and many parameters are involved to correlate the bubble coverage with current density, particularly pressure, temperature, and diffusion coefficient. The bubble coverage can be defined by the following equation:

$$\varnothing = \frac{z}{At_r}\int_0^{t_r}\pi(KR)^2 dt \tag{17}$$

where R is the bubble radius, z is the number of bubbles that simultaneously stick to the electrodes surface area A, t_r is the residence time of the bubble on the electrodes, and K is the constant related to the contact angle of bubble with electrodes, which is equal to 1 when $\vartheta \leq 90^\circ$ and equal to sin ϑ when $\vartheta \geq 90$ [22]. Integrating Eq. (17) with bubble radius R and residence time t, the following equation occurs:

$$\frac{z}{A} = \frac{2\varnothing}{\pi(KR_r)^2} \tag{18}$$

The average volume of detaching bubbles is interrelated with the rate of gas evolution and it can be expressed as follows:

$$\dot{V}_G = z\frac{V_r}{t_r} \tag{19}$$

Taking into consideration the Reynolds number of gas evolution, Schmidt number, Peclect number of mass transfer, and the partial pressure of the solvent, the final equation of the bubble coverage becomes:

$$\varnothing = \frac{3}{16}\frac{I\cdot\varepsilon_B\cdot R_e\cdot T\cdot d}{A\cdot(n/v)\cdot F_p\cdot D}\cdot F_o\cdot f_G\cdot\left(1-\frac{p_{H_2O}}{p}\right)^{-1} \tag{20}$$

Water electrolysis efficiency

The voltage efficiency is the efficiency that represents the proportion of the effective voltage required to split the water and the total voltage applied to the whole cell, which can be expressed as follows:

$$\eta_{\text{Voltaic}} = \frac{E^{\text{anode}} - E^{\text{cathode}}}{U_c} \tag{21}$$

and the faradic efficiency can be calculated by the following equation:

$$\eta_{\text{Faradic}} = \frac{\Delta G_{t,p}}{nFU_c} = \frac{E_{t,P}^{\text{Rev}}}{U_c} \tag{22}$$

and the thermal efficiency can be calculated by the following:

$$\eta_{\text{thermal}} = \frac{\Delta H_{t,p}}{nFU_c} = \frac{V_{t,P}^{\text{tn}}}{U_c} \tag{23}$$

Detailed relations for energy analysis and energy efficiency of the water electrolysis are reported in Refs. [15,23,24].

Exergy analysis is based on the conservation of energy and conservation of mass principles as well as the second law of thermodynamics. In this work, we performed our study using exergy analysis instead of energy analysis, because the energy analysis is only based on the first law of efficiency, which would not provide any meaningful reference to the best possible performance and thus may mislead the analysis, so we decided to perform our study using the second law efficiency (exergy efficiency).

The exergy can be defined as the maximum useful work that could be obtained from the system at a given state in a specified environment. The energy and exergy balance can be calculated as follows:

$$\sum_{\text{in}} En_{\text{in}}\dot{m}_{\text{in}} - \sum_{\text{in}} En_{\text{out}}\dot{m}_{\text{out}} + \sum_{k} \dot{Q}_k - \dot{W} = 0 \tag{24}$$

$$\sum_{\text{in}} Ex_{\text{in}}\dot{m}_{\text{in}} - \sum_{\text{in}} Ex_{\text{out}}\dot{m}_{\text{out}} + \sum_{k} E\dot{x}^{Q} - E\dot{x}^{W} - I' = 0 \tag{25}$$

where $\dot{m}_{\text{in}} = \dot{m}_{\text{out}}$ for a closed system, so Eqs. (24) and (25) become the following:

$$\sum_{k} \dot{Q}_k - \dot{W} = 0 \tag{26}$$

$$\sum_{k} E\dot{x}^{Q} - E\dot{x}^{W} - I' = 0 \tag{27}$$

where I' is the exergy destruction also called the irreversibility or lost work, which is the wasted work potential during a process. In a control volume, the exergy destruction can be calculated according to Gouy–Stodola theorem as follows [25,26]:

$$I' = T_{\text{amb}}\, S_{\text{gen}} \tag{28}$$

where S_{gen} and T are the entropy generation and the ambient temperature of the water electrolysis respectively.

The heat coming from the external heat source can be calculated as follows:

$$Q_{\text{cell}} = T\Delta S - Q_j \tag{29}$$

where Q_j is the heat resulting from the irreversibilities that is caused by the resistance of the electrodes and electrolyte, the charge transfer, and reactant/products transportation, this heat can be calculated as follows:

$$Q_j = I^2 R_{\text{total}} \tag{30}$$

The exergy efficiency of the water electrolysis can be calculated as follows:

$$\eta_{\text{exergy}} = \frac{\sum \dot{E}x_{\text{out,net}}}{\sum \dot{E}x_{\text{in,net}}} \tag{31}$$

The final equation for the exergy output and exergy efficiency becomes as follows [27–32]:

$$\sum \dot{E}x_{\text{out,net}} = E_{H_2} \times \dot{N}_{H_2,\text{out}} \tag{32}$$

$$\psi_{\text{exergy}} = \frac{E_{H_2} \times \dot{N}_{H_2,\text{out}}}{E_{\text{electric}} + E_{\text{heat,cell}} + E_{\text{heat},H_2O}} \tag{33}$$

which becomes:

$$\psi_{\text{exergy}} = \frac{E_{H_2} \times \dot{N}_{H_2,\text{out}}}{IV + Q_{\text{cell}}\left(1 - \frac{T_o}{T_s}\right) + Q_{H_2O}\left(1 - \frac{T_o}{T_s}\right)} \tag{34}$$

A simulation of the exergy efficiency was carried out using a list of input parameters for the water electrolysis, which is listed in Table 1:

Analysis discussion

The effect of anode and cathode resistance and the electrical circuit resistance (external and internal)

The ohmic overpotential is the voltage loss due to the resistance of water electrolysis components. Fig. 2(A) shows the effect of anode resistivity on the exergy efficiency and anode resistance. The increase of anode resistivity from 0.0002 to 0.001 Ω m decreases the exergy efficiency from 0.6838 to 0.6834. The increase of anode resistivity causes the anode

Table 1 – Simulation input parameters.

Parameter	Value
Temperature, °C	80
Exchange current density i_0, mA cm^{-2}	3.15×10^{-7}
Anode charge-transfer coefficient	0.402
Cathode charge-transfer coefficient	0.452
Limiting current density i_{lim}, mA cm^{-2}	0.03
Current density, mA cm^{-2}	700
Bubbles coverage coefficient	0.0153
Inlet electrolyte molarity, M (mol_{KOH} l^{-1})	8
Standard chemical exergy H_2, kJ mol^{-1}	236.09
Standard chemical exergy O_2, kJ mol^{-1}	3.97
Standard chemical exergy H_2O (l), kJ mol^{-1}	0.9
Standard chemical exergy H_2O (g), kJ mol^{-1}	9.50
KOH concentration, %	30
Pressure, bar	2

resistance to increase, which causes an increase in the anode irreversibility that is related to the ohmic losses. This irreversibility increase causes the exergy efficiency to drop. This results is well within an agreement with experimental data reported in Ref. [33] that show that material with high catalyst surface area enhance the performance. Fig. 2(A) also demonstrates that an increase of cathode resistivity from 0.0001 to 0.0006 Ω m decreases the exergy efficiency from 0.68381 to 0.68357 and increases the cathode resistance from 0.0001 to 0.0006 Ω. The decrease of the exergy efficiency is caused by the increase of ohmic loss, which leads to an increase of exergy destroyed (the increase of irreversibility is caused by the ohmic losses increase which is due to the rise of resistivity of the cathode material). Both electrical resistances and transport resistances cause heat generation according to the Joule's law [34] and transport phenomena [35] and thus inefficiency of the electrolysis system. Previous experiment performed by Rommal el al. [36] shows that one difficulty encountered in systems employing nickel electrodes in KOH electrolytes is the continual decrease in operating efficiency with time. The major component of this decrease is the rise in cathodic overpotential at constant cell current. It was found that the kinetic parameters of Tafel slope and exchange current density increase markedly with the decline of efficiency. Therefore, our results have demonstrated the main parameters that affect the ohmic overpotential which can enhance the exergy efficiency. Fig. 2(B) illustrates the effect of anode wire resistivity on exergy efficiency and anode resistance. The figure shows that the decrease of anode wire resistivity from 0.0001 to 0.00002 Ω m leads to an increase of exergy efficiency from to 0.6765 to 0.6830. The decrease of anode wire resistivity leads to a decrease of anode resistance which causes the ohmic losses to decrease. The decrease of the ohmic losses causes the exergy efficiency to increase. Fig. 2(B) also shows the decrease of exergy efficiency from 0.6838 to 0.6834 when the cathode wire resistivity rises from 1.5×10^{-6} to 6×10^{-6} Ω m which leads cathode resistance to increase from 0.0002 to 0.001 Ω, which is about 500% increase. The increase of cathode wire resistivity causes the ohmic losses to increase, which leads to an exergy efficiency drop.

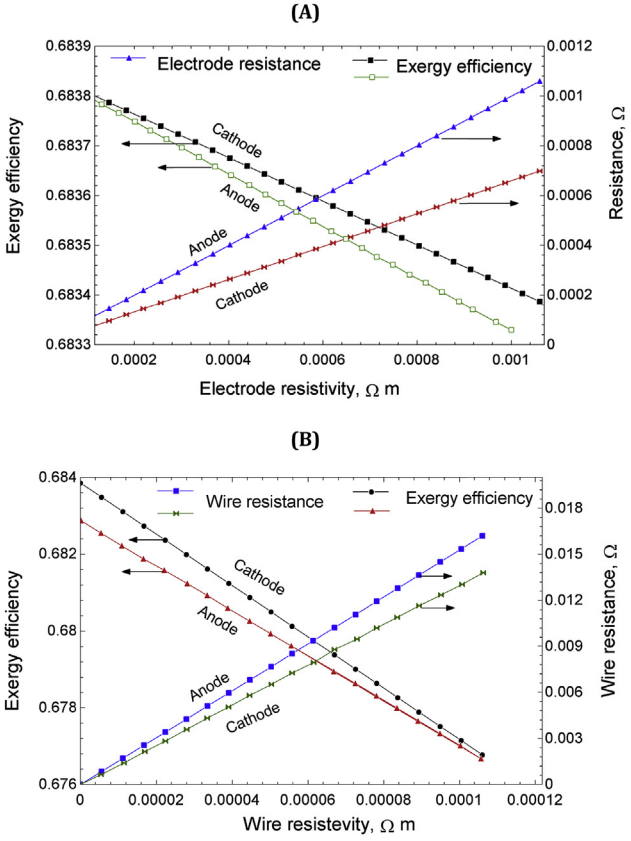

Fig. 2 – (A) The effect of electrode resistivity on the exergy efficiency and electrode resistance. (B) The effect of electrode wire resistivity on the exergy efficiency and the wire resistance.

The effect of ionic resistances

The enhancement of the ionic conductivity of the electrolyte decreases the resistance at the electrode surface. The molarity and temperature are the key variables that impact the ionic conductivity. Fig. 3(A) illustrates that increases of molarity of the aqueous KOH solution increase the ionic conductivity until it reach 8 mol l^{-1}; then it starts to decrease. Fig. 3 also demonstrates that increase of temperature enhances the ionic conductivity. Previous experiment results show that rising of the molarity improved the performance of the electrolyzer cell with the homogeneous catalyst [37]. The theoretical result reported in Fig. 3 is well within agreement with experimental data reported in Ref. [20]. The typical effect of temperature on the overpotential is summarized by Kinoshita [38], also Zeng el al. [11] has shown that an increase in temperature will result in a decrease in the overpotential at the same current density. The highest ionic conductivity was 2.5 S cm^{-1} at a temperature of 418 K and molarity of 8 mol l^{-1}. Previous experiments have demonstrated that the molarity increase of potassium hydroxide in the solution has an effect on the rust removal rate. Also the enhancement of molarity of KOH results in the removal of loose rust and grease, which is known as cathodic cleaning [39]. Fig. 3(B) illustrates that an increase of distance between the electrodes decreases the exergy efficiency, and this is caused by the increase of ionic resistance that leads to an exergy drop. Previous study done by Zeng el al. and [40] shows that a smaller gap is needed to avoid electric sparks, posing an explosion hazard. Therefore, an optimal gap between electrodes has to be identified.

Fig. 4(A) shows the effect of KOH concentration on molarity and ionic conductivity; this developed correlation demonstrates that an increase of concentration of KOH in the solution increases the molarity and ionic conductivity simultaneously. Fig. 4(B) illustrates that an increase of KOH concentration from 5% to 25% increases the exergy efficiency from 0.65 to 0.68 as well as increasing the ionic conductivity from 0.5 to 1.1 S cm^{-1}. Previous experiment results show that the optimal current density is obtained when electrolyte concentration is 20 wt% [41]. The highest increase of exergy efficiency was from 1 to 10% concentration; then it starts to slowly increase from 10% to 40% concentration. The increase of exergy efficiency is due to enhancement of the electrochemical reaction caused by the increase of ionic conductivity of the water electrolysis solution.

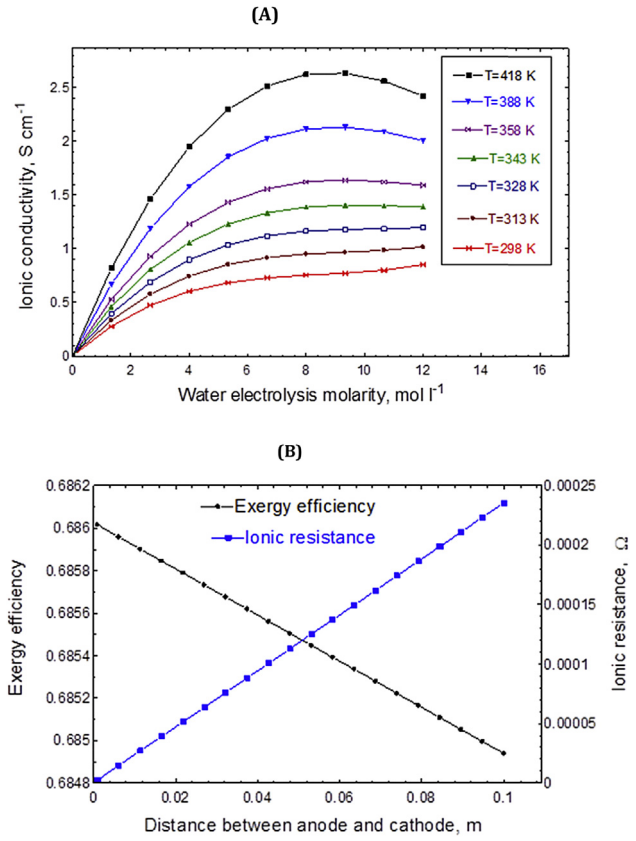

Fig. 3 – (A) The effect of electrolysis molarity on specific conductivity at various operating temperature. (B) The effect of distance between the electrodes on exergy efficiency and ionic resistance.

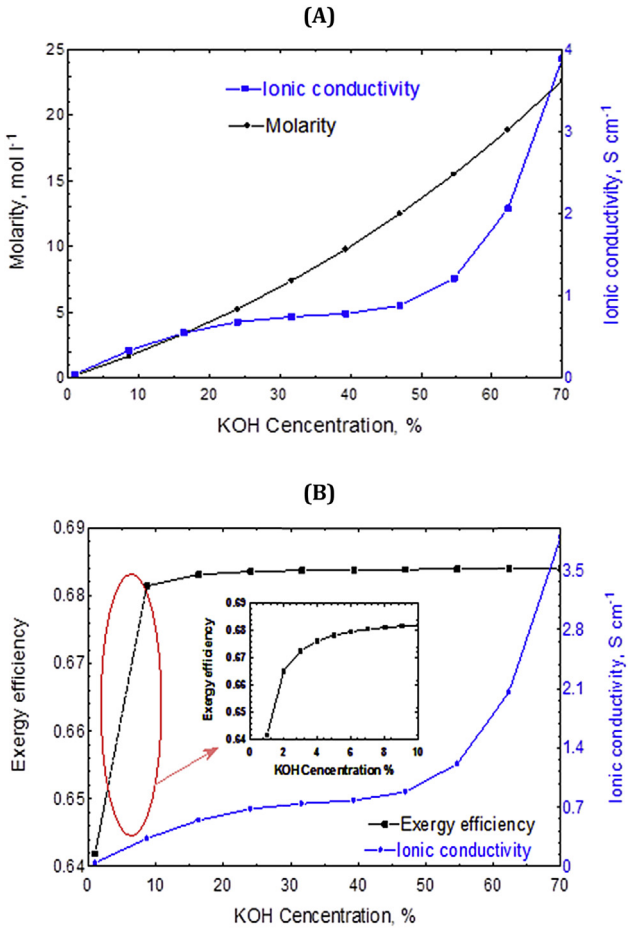

Fig. 4 – (A) The effect of weight percentage of KOH on molarity and ionic conductivity. (B) The effect of weight percentage of KOH on the ionic conductivity and exergy efficiency.

The effect of membrane resistance

The function of membrane in the alkaline water electrolysis is to allow the ions to pass through but not the gases. The membrane material must be resistant to corrosion due to the alkaline environment at elevated temperature [42,43]. Therefore, selection of membrane material must be desires for the corrosion resistance as well reducing the ohmic membrane resistance. The membrane permeability is an important parameter when it comes to design membrane for alkaline water electrolysis to allow the ions to pass through but not the gases. Previous experiment performed by Ref. [44] has shown that the membrane needs to withstand quite severe conditions, e.g., in chlor-alkali or water electrolysis. Therefore, an analysis of the membrane parameters effect on alkaline water electrolysis and its effect on exergy efficiency is desirable. Fig. 5(A) demonstrates that enhancement of the membrane permeability causes the exergy efficiency to decline. The increase of the membrane permeability enhances the apparent conductivity, which causes the membrane resistivity to decline, and this causes the rise of membrane resistance (which is part of the ohmic loss/irreversibility). Fig. 5(B) shows that an increase of membrane resistivity from 1 to 20 Ω cm causes the membrane resistance to drop from 1.2 to 0.2 Ω while increasing the exergy efficiency from 0.2 to 0.55. The increase of membrane resistivity causes the membrane resistance to drops, which enhances the electrochemical reaction of the water electrolysis. Similar results we reported in Fig. 6 using a 3D model.

The effect of oxygen and hydrogen bubbles

The oxygen bubble percentage is the percentage of bubble that covers the electrochemical surface area of the electrode. Previous experiments performed on PEM water electrolysis [3,45] shows the effect of earth gravity on the accumulation of bubbles. The results show that the accumulation of bubbles on the electrodes is smaller under normal earth gravity condition than under zero gravity. Also Olesen el al. [46] has study the effect of pressure on the bubbles for the PEM water electrolysis, the results shows that the increase of pressure induces a falling of the of mole fraction of water vapor in the product gases as the total pressure increases. Therefore, the study of the effect of bubbles on the ohmic resistance and exergy efficiency for the alkaline water electrolysis is required. Fig. 7(A) shows that an increase of oxygen bubble percentage decreases the exergy efficiency, and this is caused by an increase of bubble resistance. The shadowing rate of the electrode increases the heat generated from the water

electrolysis. During the electrolysis process, heat is evolves at the cathode and is absorbed at the anode. Also Fig. 7(A) illustrates the effect of hydrogen bubble percentage on the exergy efficiency and hydrogen resistance. The increase of hydrogen bubble from 10% to 30% on the electrode causes the bubble resistance to increase from 0.004 to 0.007 Ω, which leads to an exergy drop from 0.684 to 0.6825. Fig. 7(B) illustrates the effect of the distance between the electrodes on the exergy efficiency and ohmic resistance due to oxygen bubbles. The increase of distance between electrodes from 0.05 m to 0.1 m decrease the efficiency from 0.6855 to 0.6846 while increasing the oxygen bubble resistance from 0.0001 to 0.0003 Ω Fig. 7(B) also shows that an increase of distance between the electrodes causes the exergy efficiency to drop and the hydrogen bubble resistance to increase.

The exergy loss caused by different ohmic resistance is illustrated in Fig. 8, the results shows that the highest exergy loss is due to hydrogen bubbles followed by the electrolyte ionic resistance and oxygen bubbles resistance, respectively. The exergy loss due to wire resistance is relatively small and can be neglected. Therefore, it is important to consider the effect of hydrogen bubbles phenomena in the future of any development of the alkaline water electrolysis.

Conclusions

The theoretical and analytical study of the alkaline water electrolysis ohmic overpotential effect on exergy efficiency results shows that some of the parameters are recommended in order to reduce the ohmic overpotential and to increase the exergy efficiency and hydrogen production of the cells:

- Decreasing the distance between anode and cathode to less than 0.1 m causes the bubble and ionic resistance to drop to 0.0004 and 0.0003 Ω respectively, which leads to an increase of the exergy efficiency.
- Having the electrodes with material resistivity less than 0.002 Ω m causes the electrode ohmic resistance to drop to 0.001 Ω, and this causes the exergy efficiency to increase.
- Increasing the molarity of the electrolyte to the range of 8–10 mol l^{-1} offers the highest range of the ionic

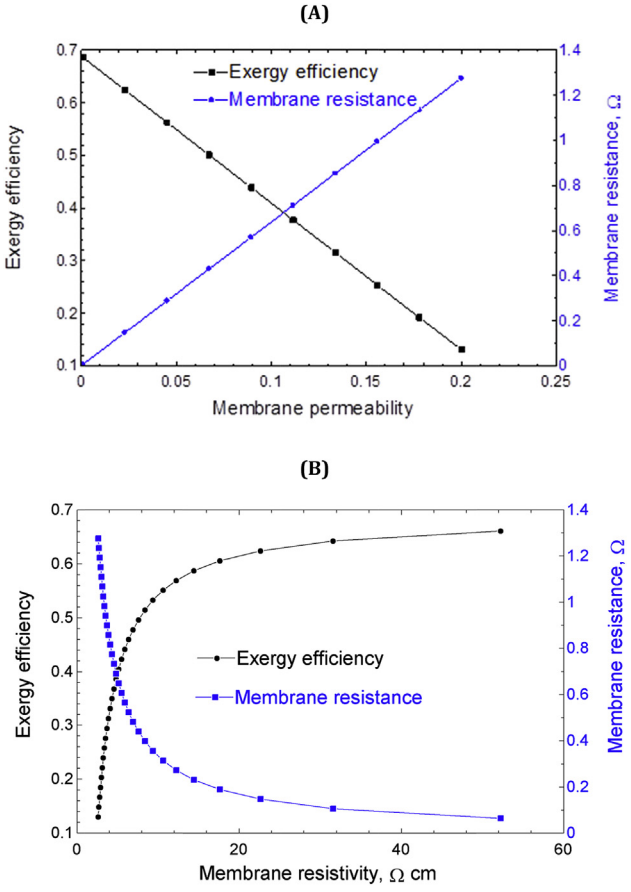

Fig. 5 – (A) The effect of membrane permeability on exergy efficiency and membrane resistance. (B) The effect of membrane resistivity on exergy efficiency and membrane resistance.

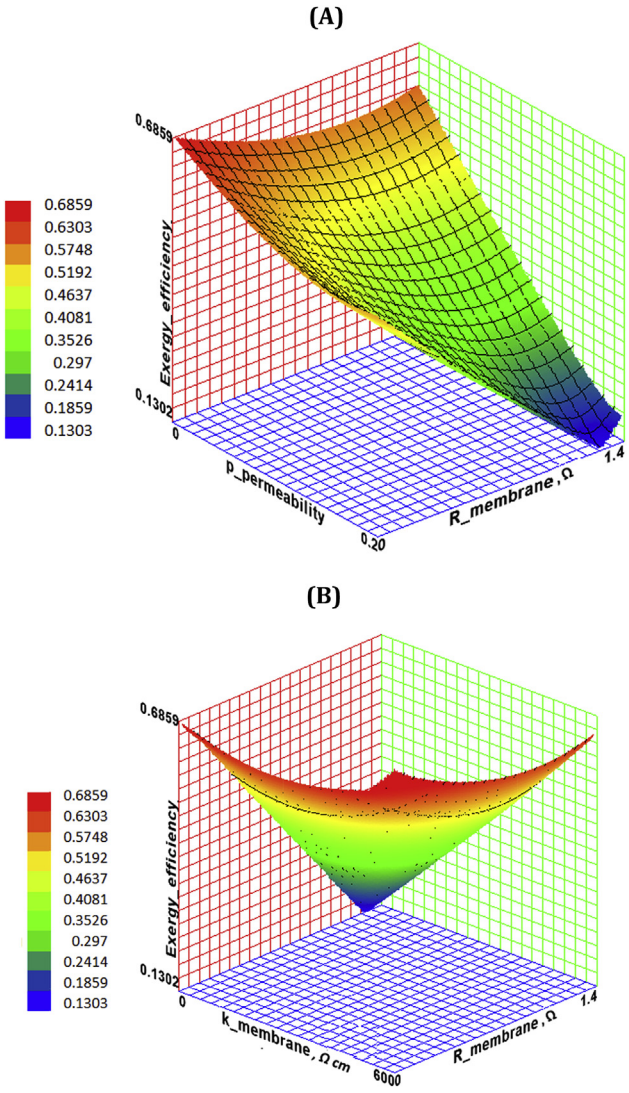

Fig. 6 – (A) The effect of membrane permeability and membrane resistance on the exergy efficiency. (B) The effect of membrane resistivity and membrane resistance on the exergy efficiency.

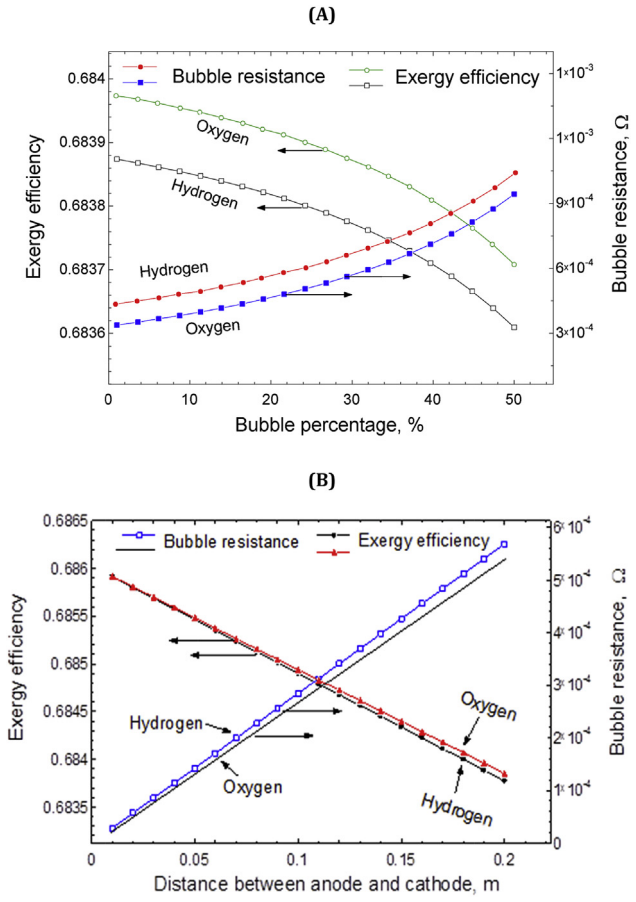

Fig. 7 – (A) The effect of bubble percentage on exergy efficiency and oxygen bubble resistance. (B) The effect of distance between anode and cathode on exergy efficiency and bubble resistance.

conductivity of the electrolyte, which causes the ionic resistance to drop and this is reflected as increase on the exergy efficiency.

- Increasing the operating temperature from 298 to 360 K increases the ionic conductivity from 0.7 to 2.5 S cm^{-1} respectively, in which causes the ionic resistance to drop and this leads to an increase of the exergy efficiency.
- Decreasing the percentage of the anode and cathode surface covered by the bubble to less than 10% reduces the bubble resistance to 4×10^{-4} and 5×10^{-4} Ω respectively, which causes the exergy efficiency to increase.
- Decrease the membrane permeability to less than 0.002 leads to the decrease of membrane resistance to 0.05 Ω which leads to an increase of exergy efficiency.

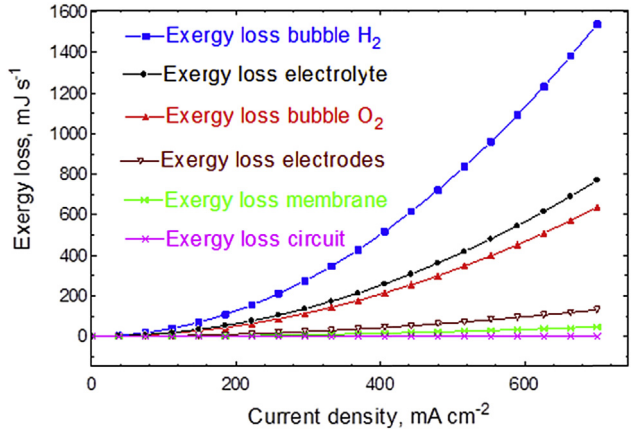

Fig. 8 – Comparison of the exergy destruction of the effect of various resistance parameters.

Finally, the highest exergy loss is caused by the hydrogen bubbles followed by the electrolyte ionic resistance and oxygen bubbles resistance, respectively. The exergy loss due to wire resistance is relatively small and can be neglected. To the authors knowledge this is the first water electrolysis model that considers the effects of materials parameters and operating condition on the exergy efficiency of the water electrolysis. Our findings offer a better understanding of the conditions required for optimum water electrolysis performance by reducing the ohmic overpotential. The use of this numerical model will help and guide researchers to focus on the key parameters that influence the ohmic polarization and overall the performance of the water electrolysis in order to provide a robust design. This model will also reduce the research and development costs by reducing the research time and the cost of the experiments and equipment.

Acknowledgment

The authors gratefully acknowledge and wish to thank Professor Jeffery Allen from Michigan Technological University for his support, help and useful comments.

Appendix A

The activation overvoltage, V_{act}, is the voltage loss that is attributed to driving the electrochemical reactions and is necessary to overcome the molecular bonds. The activation overpotential is caused by the equilibrium cell voltage, which is stated by the following equation:

$$E^{o} = E^{o}_{anode} - E^{o}_{cathode} \quad (A.1)$$

The activation overpotential can be calculated by the following:

$$\eta_{a/c} = -2.3026\frac{RT}{nF\alpha^{\bar{a}}_{c}}\log(i_o) + 2.3026\frac{RT}{nF\alpha^{\bar{a}}_{c}}\log(i) \quad (A.2)$$

And the transfer charge coefficient can be estimated as follows:

$$\alpha^{a} = 0.0675 + 0.00095T \quad (A.3)$$

$$\alpha^{c} = 0.1175 + 0.00095T \quad (r^2 = 0.9987 \text{ for Ni}) \quad (A.4)$$

The overpotential of hydrogen and oxygen can be calculated as follows:

$$\eta_{cathode} = 2.3\frac{RT}{\alpha F}\log\left(\frac{i}{i_0}\right) \quad (A.5)$$

$$\eta_{anode} = 2.3\,\frac{RT}{(1-\alpha)F}\log\left(\frac{i}{i_0}\right) \tag{A.6}$$

The relationship between the change in Gibbs free energy and equilibrium cell voltage can be calculated as follows:

$$\Delta G = nFE^{o} \tag{A.7}$$

The total energy is expressed as a thermoneutral voltage $V_{t,p}^{tn}$, which is dependent on operating pressure, temperature, and high heating value voltage $V_{t,p}^{HHV}$.

$$\Delta H_{t,p} = n\,FV_{t,p}^{tn} + \varphi(H_{t,P}^{w(l)} - H_{t_o,P_o}^{w(l)}) \tag{A.8}$$

where

$$\Delta H_{t,p} = n\,FV_{t,p}^{tn} + \varphi(H_{t,P}^{w(l)} - H_{t_o,P_o}^{w(l)}) \tag{A.9}$$

The reversible potential can be expressed by the following equation:

$$nFE_{t,P}^{Rev} = -\Delta G_{t,P} = \mu_{t,P}^{H_2} + \mu_{t,P}^{O_2} - \mu_{t,P}^{w(g)} \tag{A.10}$$

$$nFE_{t,P}^{Rev} = nFE_{t,P_o}^{Rev} + RT\ln((P-P_w)^{1.5}\frac{P_{w^*}}{P_w} \tag{A.11}$$

where the vapor pressure of pure water P_{w^*} and P_w can be calculated by the following equation:

$$P_w = T^{-3.498}\exp\left(37.93 - \frac{6426.32}{T}\right) \cdot \exp\left(0.016214 - 0.13802m + 0.19330\sqrt{m}\right) \tag{A.12}$$

$$P_{w^*} = T^{-3.498}\exp\left(37.043 - \frac{6275.32}{T}\right) \tag{A.13}$$

REFERENCES

[1] Zamfirescu C, Naterer GF, Dincer I. Water splitting with a dual photo-electrochemical cell and hybrid catalysis for enhanced solar energy utilization. Int J Energy Res 2013;37(10):1175–86.

[2] Obara S. Study of a fuel cell network with water electrolysis for improving partial load efficiency of a residential cogeneration system. Int J Energy Res 2006;30(8):567–83.

[3] Jun-Tao W, Wei-Wei W, Cheng W, Zong-Qiang M. Corrosion behavior of three bipolar plate materials in simulated SPE water electrolysis environment. Int J Hydrogen Energy 2012;37(17):12069–73.

[4] Jong-Gil O, Woong HL, Hansung K. The inhibition of electrochemical carbon corrosion in polymer electrolyte membrane fuel cells using iridium nanodendrites. Int J Hydrogen Energy 2012;37(3):2455–61.

[5] Rashmi C, Satanand S, Olusola OJ, Sudip M. A review on development of industrial processes and emerging techniques for production of hydrogen from renewable and sustainable sources. Renew Sustain Energy Rev 2013;23:443–62.

[6] Carmo M, Fritz DL, Mergel J, Stolten D. A comprehensive review on PEM water electrolysis. Int J Hydrogen Energy 22 April 2013;38(12):4901–34. ISSN 0360-3199, http://dx.doi.org/10.1016/j.ijhydene.2013.01.151.

[7] Dunn S. Hydrogen futures: toward a sustainable energy system. Int J Hydrogen Energy 2002;27:235–64.

[8] De-Souza RF, Padilha JC, Goncalves RS, De-Souza MO, Rault-Berthelot J. Electrochemical hydrogen production from water electrolysis using ionic liquid as electrolytes: towards the best device. J Power Sources 2007;164:792–8.

[9] Frank A, Christodoulos C, Mogens BM. Alkaline electrolysis cell at high temperature and pressure of 250 °C and 42 bar. J Power Sources 2013;229:2–31.

[10] Jaroslaw M, Guandalini G, Campanari S. Modeling an alkaline electrolysis cell through reduced-order and loss-estimate approaches. J Power Sources 2014;269:203–11.

[11] Zeng K, Zhang D. Recent progress in alkaline water electrolysis for hydrogen production and applications. Prog Energy Combust Sci 2010;36(3):307–26.

[12] Marini S, Salvi P, Nelli P, Pesenti R, Villa M, Berrettoni M, et al. Advanced alkaline water electrolysis. Electrochim Acta 2012;82:384–91.

[13] Djafour A, Matoug M, Bouras H, Bouchekima B, Aida MS, Azoui B. Photovoltaic-assisted alkaline water electrolysis: basic principles. Int J Hydrogen Energy 2011;36(6):4117–24.

[14] Mandin P, Derhoumi Z, Roustan H, Rolf W. Bubble over-potential during two-phase alkaline water electrolysis. Electrochim Acta 2014;128:248–58.

[15] Manabe A, Kashiwase M, Hashimoto T, Hayashida T, Kato A, Hirao K, et al. Basic study of alkaline water electrolysis. Electrochim Acta 2013;100(30):249–56.

[16] Allebrod F, Chatzichristodoulou C, Mogensen MB. Alkaline electrolysis cell at high temperature and pressure of 250 °C and 42 bar. J Power Sources 2013;229:22–31.

[17] Shen M, Bennett N, Ding Y, Scott K. A concise model for evaluating water electrolysis. Int J Hydrogen Energy 2011;36(22):14335–41.

[18] Allanore A, Lavelaine H, Valentin G, Birat JP, Delcroix P, Lapicque F. Observation and modeling of the reduction of hematite particles to metal in alkaline solution by electrolysis. Electrochim Acta 2010;55(12):4007–13.

[19] Hammoudi M, Henao C, Agbossou K, Dubé Y, Doumbia ML. New multi-physics approach for modelling and design of alkaline electrolyzers. Int J Hydrogen Energy 2012;37(19):13895–913.

[20] Gilliam RJ, Graydon JW, Kirk DW, Thorpe SJ. A review of specific conductivities of potassium hydroxide solutions for various concentrations and temperatures. Int J Hydrogen Energy 2007;32(3):359–64.

[21] Macmullin RB, Muccini GA. Characteristics of porous beds and structures. AlChE J 1956;2:393–403.

[22] Vogt H. Contribution to the interpretation of the anode effect. Electrochim Acta 1997;42(17):2695–705.

[23] Nikolic VM, Tasic GS, Maksic AD, Saponjic DP, Miulovic SM, Kaninski MPM. Raising efficiency of hydrogen generation from alkaline water electrolysis – energy saving. Int J Hydrogen Energy 2010;35(22):12369–73.

[24] Cardoso DSP, Amaral L, Santos DMF, Šljukić B, Sequeira CAC, Macciò D, et al. Enhancement of hydrogen evolution in alkaline water electrolysis by using nickel-rare earth alloys. Int J Hydrogen Energy 2015;40(12):4295–302.

[25] Kotas TJ. The exergy method of thermal plant analysis. Malabar, FL: Krieger Publish Company; 1995.

[26] Wong KFV. Thermodynamics for engineers. Boca Raton, FL: University of Miami, CRC Press LLC; 2000.

[27] Ni M, Leung MKH, Leung DYC. Energy and exergy analysis of hydrogen production by a proton exchange membrane (PEM) electrolyzer plant. Energy Convers Manag 2008;49:2748–56.

[28] Ni M, Leung MKH, Leung DYC. Energy and exergy analysis of hydrogen production by solid oxide steam electrolyzer plant. Int J Hydrogen Energy 2007;32:4648–60.

[29] Rosen M. Energy and exergy analysis of electrolytic hydrogen production. Int J Hydrogen Energy 1995;20:547–53.

[30] Kalinci Y, Dincer I, Hepbasli A. Energy and exergy analyses of a hybrid hydrogen energy system: a case study for Bozcaada. Int J Hydrogen Energy 2016. http://dx.doi.org/

10.1016/j.ijhydene.2016.02.048. Available online 16 March 2016.
[31] Balta MT, Dincer I, Hepbasli A. Thermodynamic assessment of geothermal energy use in hydrogen production. Int J Hydrogen Energy 2009;34:2925–39.
[32] Houcheng Z, Guoxing L, Jincan C. Evaluation and calculation on the efficiency of a water electrolysis system for hydrogen production. Int J Hydrogen Energy 2010;35(20):10851–8.
[33] Esswein AJ, McMurdo MJ, Ross PN, Bell AT, Tilley TD. Size-dependent activity of Co3O4 nanoparticle anodes for alkaline water electrolysis. J Phys Chem C 2009;113(33):15068–72. http://dx.doi.org/10.1021/jp904022e.
[34] Oldham KB, Myland JC. Fundamentals of electrochemical science. 1st ed. San Diego: Academic Press; 1993.
[35] Bird RB, Stewart WE, Lightfoot EN. Transport phenomena. 2nd ed. New York: John Wiley &Sons; 2007.
[36] Rommal HEG, Moran PJ. Time-dependent energy efficiency losses at nickel cathodes in alkaline water electrolysis systems. J Electrochem Soc 1985;32(2):325–9. http://dx.doi.org/10.1149/1.2113831.
[37] Bonino CA, Concepcion JJ, Trainham JA, Meyer TJ, Newmana J. Water electrolysis with a homogeneous catalyst in an electrochemical cell. J Electrochem Soc 2013;160(10):F1143–50.
[38] Kinoshita K. Electrochemical oxygen technology. 1st ed. New York: John; 1992.
[39] Boudenne JL, Cerclier O, Galéa J, Vlist EVD. Electrochemical oxidation of aqueous phenol at a carbon black slurry electrode. Appl Catal A General 1996;143(2):185–202.
[40] Nunes SP, Peinemann KV. Membrane technology. 2nd ed. Weinheim: Wiley- VCH Verlag GmbH & KGaA; 2007.
[41] Ming-Yuan L, Lih-Wu H. Effects of magnetic field and pulse potential on hydrogen production via water electrolysis. Int J Energy Res 2014;38(1):106–16.
[42] Rosa VM, Santos MBF, Dasilva EP. New materials for water electrolysis diaphragms. Int J Hydrogen Energy 1995;20:697–700.
[43] Hickner MA, Ghassemi H, Kim YS, Einsla BR, McGrath JE. Alternative polymer systems for proton exchange membranes (PEMs). Chem Rev 2004;104:4587–612.
[44] Protopopoff E, Marcus P. Poisoning of the cathodic hydrogen evolution reaction by sulfur chemisorbed on platinum. Electrochem Soc 1988;135(12):3071–3.
[45] Siracusano S, Baglio V, Briguglio N, Brunaccini G, Blasin AD, Stassi A, et al. An electrochemical study of a PEM stack for water electrolysis. Int J Hydrogen Energy 2012;37(2):1939–46.
[46] Olesen AC, Rømer C, Kær SK. A numerical study of the gas-liquid, two-phase flow mal distribution in the anode of a high pressure PEM water electrolysis cell. Int J Hydrogen Energy 2016;41(1):52–68.